Automatic Recognition of Soybean Leaf Diseases Using UAV Images and Deep Convolutional Neural Networks

Everton Castelão Tetila, Bruno Brandoli Machado, Gabriel Kirsten Menezes, Adair da Silva Oliveira, Jr., Marco Alvarez, Willian Paraguassu Amorim, Nícolas Alessandro de Souza Belete, Gercina Gonçalves da Silva, and Hemerson Pistori

***Abstract*— Plant diseases are a crucial issue in agriculture. An accurate and automatic identification of leaf diseases could help to develop an early response to reduce economic losses. Recent research in plant diseases has adopted deep neural networks. However, such research has used the models as a black-box passing the labeled images through the networks. This letter presents an analysis of the network weights for the automatic recognition of soybean leaf diseases applied to images taken straight from a small and cheap unmanned aerial vehicle (UAV). To achieve high accuracy, we evaluated four deep neural network models trained with different parameters for fine-tuning (FT) and transfer learning. Data augmentation and dropout were used during the network training to avoid overfitting. Our methodology consists of using the SLIC method to segment the plant leaves in the top-view images obtained during the flight. We tested our data set created from real flight inspections in an end-to-end computer vision approach. Results strongly suggest that the FT of parameters substantially improves the identification accuracy.**

***Index Terms*— Aerial imagery, deep learning, precision agriculture, soybean leaf diseases, unmanned aerial vehicle (UAV)-based remote sensing.**

I. Introduction

COMPUTER vision has been widely used as a precision farming tool to increase grain production. It is estimated that the world population growth will reach 9.7 billion by 2050 and 11.2 billion by 2100 [1], which means that it will be necessary to substantially expand the amount of food produced. Unmanned aerial vehicles (UAVs) have helped to innovate grain production. They are equipped with high-resolution space cameras and are capable of capturing high-definition images while flying over a plantation a few meters high. This allows automatic systems to monitor the cultivation and harvesting of entire crop farms. In addition, UAVs in crop field have been considered as a vital element to identify foliar disease patches, allowing farmers and specialists to make better management decisions.

The recognition of diseases in the early visual stages of epidemics allows more efficient management of inputs since the diseases can present different susceptibilities to the active principle of the same pesticide. In addition, identification of diseases in the field is important for the planning of the next soybean crop. Regular planting inspections are also difficult to perform when cultivating in large areas. To overcome these problems, there is a growing motivation to use VANTs in agriculture as they are able to fly over fields in data collection missions, making it feasible the use of computer vision systems to identify diseases that affect crops in different cultivars.

Remote sensing methods using different types of optical technologies have been proposed to capture field images in specific spectral bands to increase agricultural productivity. Image technologies include RGB [2], thermography sensors [3], chlorophyll fluorescence [4], LiDAR [5], and multi-hyperspectral cameras [6]. In order to process and analyze the collected images, machine learning methods [7] were proposed to detect plant diseases [8], [9] in various cultures, using images in which background illumination and reflection can be well controlled. However, a limited number of studies have addressed the use of images captured by UAVs to identify soybean diseases in the field. In this context, remote images based on UAVs and machine learning methods were proposed to identify diseases in soybean [10], [11].

In recent years, the convolutional neural network (CNN) models have become popular because of the impressive results in image classification problems. Tan *et al.* [12] proposed a neural network to identify diseases in soybean seeds. Mohanty *et al.* [9] and Sladojevic *et al.* [13] trained different approaches of CNNs to classify images of diseases in

Manuscript received April 9, 2019; revised June 27, 2019; accepted July 23, 2019. *(Corresponding author: Everton Castelão Tetila.)*

E. Castelão Tetila is with the Faculty of Exact Sciences and Technology, Federal University of Grande Dourados, Dourados 79825-070, Brazil, and also with the Postgraduate Program in Local Development, Dom Bosco Catholic University, Campo Grande 79117-010, Brazil (e-mail: evertontetila@ufgd.edu.br).

B. Brandoli Machado, G. K. Menezes, A. d. S. Oliveira, Jr., G. G. da Silva, and H. Pistori are with the Faculty of Computing, Federal University of Mato Grosso do Sul, Campo Grande 79070-900, Brazil, and also with the Postgraduate Program in Local Development, Dom Bosco Catholic University, Campo Grande 79117-010, Brazil.

M. Alvarez is with the Department of Computer Science and Statistics, University of Rhode Island, Kingston, RI 02881 USA.

W. P. Amorim is with the Faculty of Exact Sciences and Technology, Federal University of Grande Dourados, Dourados 79825-070, Brazil.

N. A. d. S. Belete is with the Postgraduate Program in Local Development, Dom Bosco Catholic University, Campo Grande 79117-010, Brazil, with the Production Engineering Department, Federal University of Rondônia, Cacoal 76801-016, Brazil, and also with the Faculty of Engineering, University of Porto, 4099-002 Porto, Portugal.

Color versions of one or more of the figures in this letter are available online at http://ieeexplore.ieee.org.

Digital Object Identifier 10.1109/LGRS.2019.2932385

different plant species; however, the images were collected under controlled conditions. Similarly, a CNN was used in [14] to classify three different legume species (white beans, red beans, and soybeans) from the leaf vein patterns. In all the cited works, the leaf images were previously cut in the field and captured by a camera in the laboratory.

Deep neural networks and images captured in real field conditions under different lighting conditions, objects size, and background variations were proposed in [15] to detect nine different types of diseases and pests in tomato plants and in [16] to detect diseases in 25 plant species, thus avoiding the process of collecting and analyzing samples in the laboratory. Despite this, the authors used images collected by digital cameras, rather than aerial images captured by UAVs, which makes it difficult to perform regular inspections in the field when the cultivation areas are large. In addition, no studies were found in the literature that address deep learning models using UAVs images to detect and classify soybean diseases in real field conditions. We also did not find experiments comparing different parameters for fine-tuning (FT) and transfer learning (TL) with state-of-the-art deep learning models.

This letter evaluates four deep learning models for the automatic recognition of soybean leaf diseases, using images captured 2 m above the plantation with a DJI Phantom 3 Professional. Initially, we considered an image segmentation step using the SLIC superpixels method [17] to segment the plant leaves in the images obtained during the flight inspection. Then an agronomist labeled each soybean leaf image in a specific disease class to describe examples of each class. The proposed evaluation approach uses an image data set divided into six classes. Accuracy, training time, and learning error of the deep learning models are evaluated in the task of recognizing soybean leaf diseases. These diseases are usually present in several producing regions of the world, causing loss of yield in several cultivars, such as corn, soybean, wheat, and beans.

II. Proposed Approach

In this section, we present a computer vision system to identify soybean diseases from images collected by the UAV. The proposed approach adopts the SLIC superpixels method to segment plant leaves in the captured images. The SLIC algorithm was chosen because it is faster with linear complexity, it has more memory efficient than methods based on superpixels, and it yields state-of-the-art adherence to image boundaries, which outperforms existing methods when used for image segmentation, according to the comparison made in [17].

SLIC superpixels employ the k-means [18] algorithm for the generation of similar regions, called superpixels. The parameter k refers to the number of superpixels in the image and allows to control the size of superpixels. SLIC groups regions of pixels in the 5-D space defined by l, a, b (values of the CIELAB color scale), and the coordinates x and y of the pixels. An input image is segmented into regular regions, defining the number k of superpixels with approximately (N/k) pixels, where N is the number of pixels in the image.

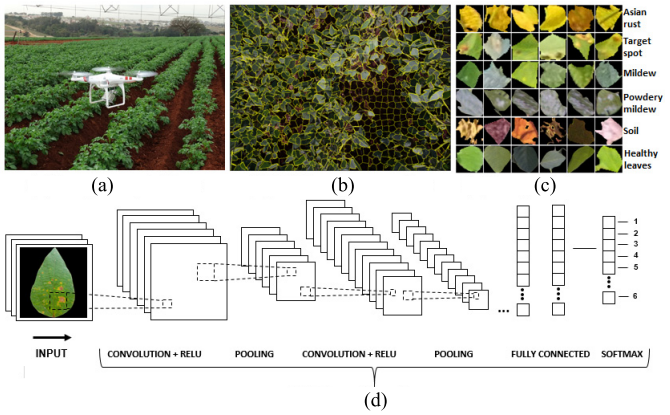

Fig. 1. Proposal of a computer vision system to identify soybean leaf diseases with UAV images. (a) Image acquisition. (b) SLIC segmentation. (c) Image data set. (d) Classification.

Each region composes an initial superpixel of dimensions $S \times S$, where $S = ((N/k))^{1/2}$. The centers of the superpixel clusters $C_k = [l_k, a_k, b_k, x_k, y_k]$ with $k = [1, k]$ are sampled on a regular grid spaced S pixels apart. The centers are moved to the lowest gradient position in a 3×3 neighborhood, avoiding the allocation of centroids on an edge and to reduce the chance of seeding a superpixel with a noisy pixel. Each pixel is associated with the nearest cluster center; an update step adjusts the cluster centers to be the mean $labxy$ vector of all the pixels belonging to the cluster [17].

A schematic of the proposed approach is shown in Fig. 1. It illustrates the proposed system that consists of four steps: 1) image acquisition; 2) SLIC segmentation; 3) image data set; and 4) classification of foliar diseases. Initially, flight inspection was conducted with the UAV in the soybean fields to capture images of the plantation [see Fig. 1(a)]. These images were segmented using the SLIC superpixels method [Fig. 1(b)]. After segmentation of the image, leaf segments were visually analyzed by a specialist to compose a data set of superpixel images for training and testing the system, see Fig. 1(c). In this case, each superpixel was visually labeled by an agronomist into a specific class: Asian rust, target spot, mildew, powdery mildew, soil (exposed and straw), or healthy leaf samples. Subsequently, a CNN was trained to extract visual resources of superpixel images and finally to classify images of soybean diseases (see Fig. 1(d). In the postprocessing stage, the computer vision system shows the visual and quantitative results when classifying the segments of an image of the plantation. This makes it possible to calculate the disease infestation level of each planting area, allowing more efficient management of pathogens in the field.

III. Materials and Methods

A. Image Acquisition

The images of the soybean plants were captured with the Phantom 3 Professional UAV, equipped with a 1/2.3-in Sony EXMOR sensor and 12.3-Mpixel resolution. Digital negative (DNG) images were captured on the targets of interest 2 m above the plantation, using a 90° angle (right angle) of the

camera in relation to the ground. Targets of interest correspond to disease-infested areas that were identified in the field by the agronomist during flight inspection. In this case, we chose 2 m because smaller values cause plant displacement due to the wind generated by the rotor blades, which substantially modifies the initial position of the leaves. On the other hand, at higher values the leaf size in the image gets gradually reduced and, consequently, the image resolution decreases, as reported in [10].

Images were captured under real field condition from an agricultural soybean area located in the city of Dourados-MS, Brazil, with geographical coordinates 22°6'22.77" South latitude and 54°15'20.05" West longitude. A total of 300 aerial images were collected in different days and climatic conditions, during the phenological stages R1–R6 of the soybean reproductive phase. For this reason, the images captured by the UAV contain several undesired variations, such as different lighting and reflection conditions, size and position of objects, leaf movement, occlusion, background variations, and soybean phenological stages. These variations in real field conditions contribute to the system operating in a real scenario.

TABLE I

PERFORMANCE METRICS USED TO EVALUATE DEEP LEARNING MODELS

Model	Strategy	Training time (s)	Accuracy (%)	Learning error
Inception-v3	FT 100%	2558,91	98.87	0.0523
Inception-v3	FT 75%	2026,29	**99.04**	0.0490
Inception-v3	FT 50%	1812,23	97.22	0.1052
Inception-v3	FT 25%	1606,61	94.78	0.1645
Inception-v3	TL	1474,77	86.85	0.3869
Inception-v3	No TL	2558,97	95.75	0.1476
Resnet-50	FT 100%	3045,23	98.96	0.0414
Resnet-50	FT 75%	2392,65	**99.02**	0.0459
Resnet-50	FT 50%	2000,82	98.96	0.0421
Resnet-50	FT 25%	1759,21	98.79	0.0544
Resnet-50	TL	1493,96	96.95	0.1282
Resnet-50	No TL	3048,31	96.54	0.1106
VGG-19	FT 100%	3926,62	**99.02**	0.0476
VGG-19	FT 75%	3302,91	98.33	0.0569
VGG-19	FT 50%	2535,51	98.27	0.0703
VGG-19	FT 25%	1945,43	96.37	0.1236
VGG-19	TL	1736,97	77.53	0.6501
VGG-19	No TL	3904,94	69.59	0.6855
Xception	FT 100%	4548,38	**98.56**	0.0549
Xception	FT 75%	3009,02	97.98	0.0796
Xception	FT 50%	2693,55	94.53	0.2356
Xception	FT 25%	2352,87	92.63	0.2700
Xception	TL	2000,16	86.69	0.3922
Xception	No TL	4371,06	97.87	0.0796

B. UAV Height and Leaf Segmentation

To identify the leaves of the plants in the images, each plantation image was segmented using the superpixel method, according to the parameters k and m that best adjusts the segmentation of individual leaves. For our experiments, the value of $k = 2000$ was adjusted to divide an image of the plantation into 2000 segments of superpixels. This value corresponds to the average size of the segmentation of a leaf area. The value of $m = 10$ was found by adhering to the compactness limits of the superpixel segments of the SLIC algorithm.

Each image has a dimension of 4000×3000 pixels, totaling 12 000 000 pixels. An individual soybean leaf at 2 m high has about 6000 pixels. Thus, the segmentation parameter k has been defined for 2000 regions; dividing 12 000 000 pixels by 2000 regions, we get 6000 pixels for each leaf. In addition, between the phenological stages R1 and R6 that are reproductive phases of high disease incidence in soybean, there was no significant variation in leaf size. Thus, we maintain the same values of the parameters k and m found in the SLIC algorithm. As a result, 3000 superpixels images, including 500 images for each class, were distributed among the six classes of soybean disease, soil, and healthy leaves. Fig. 1(c) describes examples of each class.

C. Classification Evaluation

For image classification, deep learning models are trained with labeled images in order to learn how to identify and classify them according to visual patterns. We used an open-source implementation comprising CNNs, including Inception-v3 [19], VGG-19 [20], ResNet-50 [21], and Xception [22], which are provided as part of the Keras module and it was recognized as validation on ImageNet. Keras implementation parameters were not varied to compare the deep learning models without adjustment. We used supervised learning models with training and test sets divided into 70% for training and 30% for testing. Three metrics were used to evaluate the performance of each model: accuracy, training time, and learning error. To analyze if the models differ statistically with regard to their performance, we used the ANOVA hypothesis test. We report the p-values found for each metric and the significance level required to discard the null hypothesis.

In the experiments, we used the following input parameters. The input image width and height were equally set in 256. The batch size was set 16 images for training and the number of epochs was used 50, once the convergence was in a few iterations. We used the SGD optimizer with learning rate of 0.0001 and momentum of 0.9 (accelerate SGD in the relevant direction and dampens oscillations). The proposed approach uses a set of 500 images per class, which may not be enough to train a deep learning model. Thus, the data set was subjected to the data augmentation technique to increase the amount of data by applying rotation, rescaling, scrolling, and zooming operations. This technique aims to reinforce the rotation invariance and scale invariance in the classification task since the images are captured by the UAV at different positions and scales. The dropout rate used in the experiments was fixed at 50%. We also kept the same parameters for the data augmentation, that is, rescale of 1./255, meaning the multiplication factor for each pixel of the image, with horizontal flip, fill mode nearest (points outside the input limits are filled according to the nearest direction), zoom range of 0.3 factor, width shift range of 0.3 for horizontal and vertical shift factors, and rotation range of 30.

In order to statistically evaluate the potential of the models for the identification of diseases in soybean fields, we defined four different training strategies using FT with the weights obtained from ImageNet ranging from 25% to 100%, with a 25% step, to the network layers. We also trained the complete network with the weights initialized randomly (No TL), in addition to the TL strategy with the weights obtained from ImageNet.

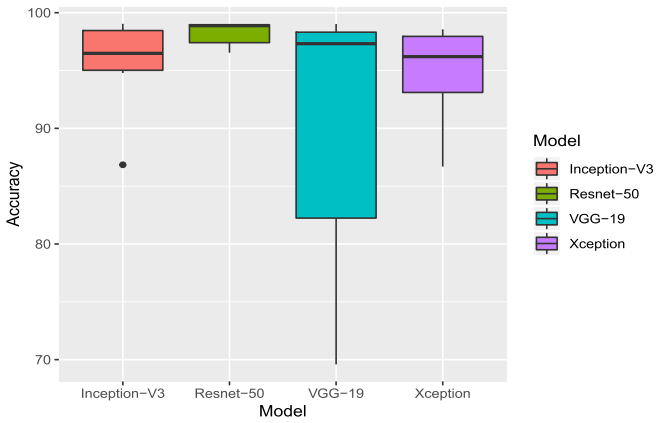

Fig. 2. Boxplot diagram comparing the accuracy results of each deep learning model.

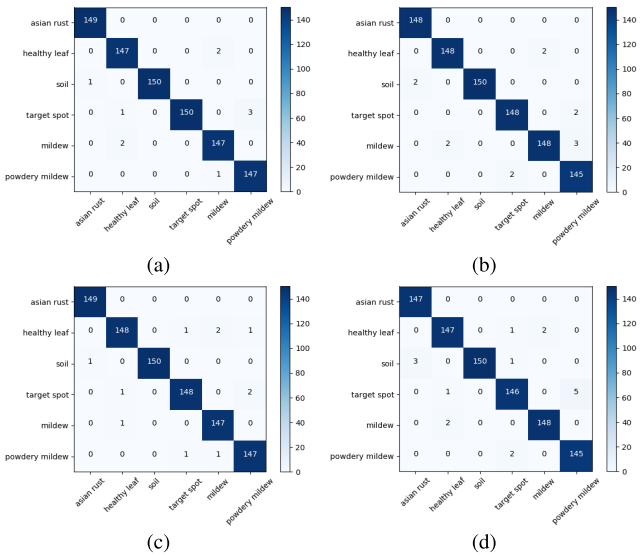

Fig. 3. Confusion matrix of the deep learning models. (a) Inception-v3. (b) Resnet-50. (c) VGG-19. (d) Xception.

In all our experiments we used a workstation with a Processor Intel Core i7-6800 K 3.40 GHz 15 MB (6N, 12T), Graphics Card Geforce GTX 1070 8 GB 1920 cuda cores, RAM memory 16 GB Kingston DDR4 2400 MHz, and Storage SSD 120 GB 2.5"SATA III Kingston Ultravalue 400.

IV. Results and Discussion

Table I shows the accuracy results obtained by the deep learning models. The highest value of accuracy obtained by each model is highlighted in the table. Table I also shows the learning error and the total training time, in seconds, to construct the classification model. The time results of Table I refer to the hardware specifications presented in Section III. Executions in different machine configurations may interfere in the results presented.

In our experiments, the Inception-v3 FT 75% model obtained the highest value of accuracy (99.04%), followed by Resnet-50, VGG-19 (99.02%), and Xception (98.56%). Inception-v3 also obtained less training time, followed by Resnet-50, VGG-19, and Xception. Through the ANOVA test,

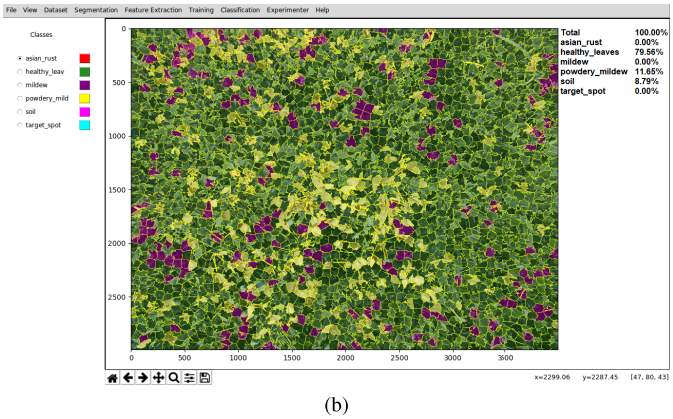

Fig. 4. Validation of our computer vision approach on a soybean crop field. (a) Aerial image taken at 2 m high using the UAV Phantom 3. In the image center, there is a powdery mildew patch in grayish color. (b) Screenshot of our computer vision system. The system presents the leaf image segmentation step and the superpixels classification using the Inception-v3 model. Color labels represent the categories for our problem.

we find the p-value of 0.412, and therefore we have no evidence that there is a statistically significant difference in the mean performance of the models tested at a significance level of 5% using accuracy as metric. On the other hand, it is important to highlight the implications of choosing a deep learning model and a strategy for training. For example, in Table I the VGG-19 model trained without TL obtained accuracy of 69.59% versus 99.02% using FT 100%, resulting in a difference of 29.43%. In addition, FT 100% and 75% strategies showed higher classification rates compared with other training strategies but obtained long training times because more layers are retrained using these strategies.

Fig. 2 shows the range of performance variation obtained by each model, with the median value highlighted in the boxplot diagram. According to the figure, Resnet-50 presented the highest value for the median and data dispersion in the best range of values for accuracy in comparison to the other models.

Fig. 3 presents the confusion matrix of the deep learning models. According to the figure, the classes target spot, powdery mildew, and healthy leaf; mildew obtained the highest number of instances classified incorrectly, due to the greater similarity of the visual patterns existing among these classes. Initial symptoms of mildew are bright green spots of 3–5 mm

on the top of the leaf that are difficult to discriminate from the healthy leaf. The lesions of the target spot begin with brown dots, with yellowish halo, evolving to large circular spots of light brown to dark brown color, reaching up to two centimeters in diameter. Powdery mildew presents a thin white covering on the leaves due to the white color of the fungus, but it changes to a grayish-brown color over time [23].

Fig. 4(b) shows the final step of the computer vision system classifying the segments of an image of the plantation captured by the UAV at 2 m high. Here, we use a practical approach with the SLIC method for image segmentation and the Inception-v3 FT 75% model for segment classification. In the postprocessing stage, a colored map is generated by providing one class per segment. The visual result of each class is highlighted in the image by the color it represents, and the quantitative result shows the level of infestation per class.

The computational complexity of the segmentation process, based on the SLIC algorithm, limits the search space to a region proportional to the superpixel size. This reduces the linear complexity to the number of superpixels k, instead of the number of pixels n. In the classification process, the system scans the image from left to right and top to bottom, classifying each superpixel individually, while providing the color of the class simultaneously. In this process, linear complexity is also proportional to the number of superpixels k.

V. Conclusion

In this letter, we evaluated four deep learning models for the task of recognizing soybean leaf diseases, using UAV images captured 2 m above the plantation. We considered an image segmentation step with the SLIC superpixels algorithm to detect plant leaves in the images. In the classification step, we compared four well-known deep learning models in the literature: Inception-v3, Resnet-50, VGG-19, and Xception. Experimental results showed that deep learning models lead to high classification rates, reaching an accuracy of up to 99.04%. In addition, in our experiments, FT 100% and 75% strategies showed higher classification rates compared with other training strategies. The results indicate that the models evaluated can support farmers in the monitoring of soybean diseases. We also demonstrate how a deep learning model can be implemented in a computer vision system to operate in a real field setting, under different lighting conditions, object size, and background variations. As part of the future work, we intend to evaluate our approach with higher resolution and multi-hyperspectral cameras.

Acknowledgment

The authors would like to thank the National Center for Scientific and Technological Development (CNPq), the Coordination for the Improvement of Higher Education Personnel (CAPES), NVIDIA Corporation, and the Foundation to Support the Development of Teaching, Science and Technology of the State of MS (FUNDECT).

References

[1] "Population division. World population prospects: The 2017 revision, key findings and advance tables," U.S. Dept. Econ. Social Affairs, New York, NY, USA, Working Paper ESA/P/WP/248, 2017.

[2] R. Diello *et al.*, "Local descriptors for soybean disease recognition," *Comput. Electron. Agricult.*, vol. 125, pp. 48–55, Jul. 2016.

[3] E.-C. Oerke, U. Steiner, H.-W. Dehne, and M. Lindenthal, "Thermal imaging of cucumber leaves affected by downy mildew and environmental conditions," *J. Exp. Botany*, vol. 57, no. 9, pp. 2121–2132, May 2006.

[4] A.-K. Mahlein, E.-C. Oerke, U. Steiner, and H.-W. Dehne, "Recent advances in sensing plant diseases for precision crop protection," *Eur. J. Plant Pathol.*, vol. 133, no. 1, pp. 197–209, May 2012.

[5] U. Weiss, P. Biber, S. Laible, K. Bohlmann, and A. Zell, "Plant species classification using a 3D LIDAR sensor and machine learning," in *Proc. 9th Int. Conf. Mach. Learn. Appl.*, Dec. 2010, pp. 339–345.

[6] V. Chelladurai, K. Karuppiah, D. S. Jayas, P. G. Fields, and N. D. G. White, "Detection of callosobruchus maculatus (F.) infestation in soybean using soft X-ray and NIR hyperspectral imaging techniques," *J. Stored Products Res.*, vol. 57, pp. 43–48, Apr. 2014.

[7] S. Sankaran, A. Mishra, R. Ehsani, and C. Davis, "A review of advanced techniques for detecting plant diseases," *Comput. Electron. Agricult.*, vol. 27, no. 1, pp. 1–13, Jun. 2010.

[8] S. Shrivastava and D. S. Hooda, "Automatic brown spot and frog eye detection from the image captured in the field," *Amer. J. Intell. Syst.*, no. 4, no. 2, pp. 131–134, 2014.

[9] S. P. Mohanty, D. P. Hughes, and M. Salathé, "Using deep learning for image-based plant disease detection," *Frontiers Plant Sci.*, vol. 7, p. 1419, Sep. 2016.

[10] E. C. Tetila, B. B. Machado, N. A. de S. Belete, D. A. Guimarães, and H. Pistori, "Identification of soybean foliar diseases using unmanned aerial vehicle images," *IEEE Geosci. Remote Sens. Lett.*, vol. 14, no. 12, pp. 2190–2194, Dec. 2017.

[11] C. Brodbeck, E. Sikora, D. Delaney, G. Pate, and J. Johnson, "Using unmanned aircraft systems for early detection of soybean diseases," in *Proc. 11th Eur. Conf. Precis. Agricult. (ECPA)*, vol. 8, no. 2, 2017, pp. 802–806.

[12] T. Kezhu, C. Yuhua, S. Weixian, and C. Xiaoda, "Identification of diseases for soybean seeds by computer vision applying BP neural network," *Int. J. Agricult. Biol. Eng.*, vol. 7, no. 3, pp. 43–50, Jun. 2014.

[13] S. Sladojevic, M. Arsenovic, A. Anderla, D. Culibrk, and D. Stefanovic, "Deep neural networks based recognition of plant diseases by leaf image classification," *Comput. Intell. Neurosci.*, vol. 2016, May 2016, Art. no. 3289801.

[14] G. L. Grinblat, L. C. Uzal, M. G. Larese, and P. M. Granitto, "Deep learning for plant identification using vein morphological patterns," *Comput. Electron. Agricult.*, vol. 127, pp. 418–424, Sep. 2016.

[15] F. Alvaro, Y. Sook, K. Sang, and P. Dong, "A robust deep-learning-based detector for real-time tomato plant diseases and pests recognition," *Sensors*, vol. 17, no. 9, p. 2022, 2017.

[16] K. P. Ferentinos, "Deep learning models for plant disease detection and diagnosis," *Comput. Electron. Agricult.*, vol. 145, pp. 311–318, Feb. 2018.

[17] R. Achanta, A. Shaji, K. Smith, A. Lucchi, P. Fua, and S. Süsstrunk, "SLIC superpixels compared to state-of-the-art superpixel methods," *IEEE Trans. Pattern Anal. Mach. Intell.*, vol. 34, no. 11, pp. 2274–2282, Nov. 2012.

[18] R. M. Haralick, "Statistical and structural approaches to texture," *Proc. IEEE*, vol. 67, no. 5, pp. 786–804, May 1979.

[19] C. Szegedy, V. Vanhoucke, S. Ioffe, J. Shlens, and Z. Wojna, "Rethinking the inception architecture for computer vision," in *Proc. IEEE Conf. Comput. Vis. Pattern Recognit.*, Jun. 2016, pp. 2818–2826.

[20] K. Simonyan and A. Zisserman, "Very deep convolutional networks for large-scale image recognition," 2014, *arXiv:1409.1556*. [Online]. Available: https://arxiv.org/abs/1409.1556

[21] K. He, X. Zhang, S. Ren, and J. Sun, "Deep residual learning for image recognition," in *Proc. IEEE Conf. Comput. Vis. Pattern Recognit.*, Jun. 2016, pp. 770–778.

[22] F. Chollet, "Xception: Deep learning with depthwise separable convolutions," in *Proc. IEEE Conf. Comput. Vis. Pattern Recognit. (CVPR)*, Honolulu, HI, USA, Jul. 2017, pp. 1800–1807.

[23] Empresa Brasileira de Pesquisa Agropecuária, *Manual de identificação de doenças de soja*, 5th ed. Londrina, Brazil: Embrapa Soja (in Portuguese), 2014.